

DUCTILITY AND STRENGTH OF REINFORCED CONCRETE COLUMNS
WITH SPIRALS OR HOOPS UNDER SEISMIC LOADING

R. Park^I, M.J.N. Priestley^{II}, W.D. Gill^{III}, R.T. Potangaroa^{IV}

SUMMARY

Eight reinforced concrete columns were tested under simulated seismic loading. The transverse reinforcement consisted of spirals or rectangular hoops. The columns were loaded axially and by cyclic horizontal loading up to displacement ductility factors of greater than 6, to study the effect of quantity of transverse reinforcement and the axial load level on the ductility and strength of the columns. The transverse reinforcement was designed according to the provisions of the draft New Zealand Concrete Design Code. The measured load-deflection hysteresis loops were relatively stable and showed only small degradation of flexural strength.

INTRODUCTION

Inelastic response of bridge structures to seismic attack will generally involve plastic hinging of the columns of the supporting piers. For frame buildings, current design philosophy is directed towards ensuring the formation of plastic hinges in the beams, rather than in the columns, but plastic hinges will need to form at the column bases and plastic hinges may form elsewhere in columns during extreme events. The amount and distribution of transverse steel necessary to ensure adequate ductility of columns without significant strength degradation is still a matter of some controversy. This paper summarises an investigation which assessed the confinement provisions of the draft New Zealand Concrete Design Code (1). Full details of the study may be seen elsewhere (2,3).

REVISED DRAFT NEW ZEALAND CONCRETE DESIGN CODE PROVISIONS

According to the revised draft of the New Zealand Concrete Design Code the potential plastic hinge region should be considered to extend over the end length of column not less than the larger of the column diameter in the case of a circular column or the longer column cross section dimension in the case of a rectangular column, or where the moment exceeds 0.8 of the maximum moment at that end of the member. An exception is that when $P_e > \phi 0.3f'_c A_g$, the above length should be increased by 50%.

In the potential plastic hinge region the maximum centre to centre spacing of the transverse reinforcement should not be less than the larger of one-fifth of the column diameter or one-fifth of the smaller column cross section dimension, or six longitudinal bar diameters, or 200 mm. When spirals or circular hoops are used, ρ_s should not be less than the smaller of

$$\rho_s = 0.45 \left(\frac{A_g}{A_c} - 1 \right) \frac{f'_c}{f_{yh}} \left(0.5 + 1.25 \frac{P_e}{\phi f'_c A_g} \right) \quad (1)$$

I Professor of Civil Engineering, University of Canterbury, New Zealand.

II Reader in Civil Engineering, University of Canterbury, New Zealand.

III Assistant Engineer, Ministry of Works and Development, New Zealand.

IV Assistant Engineer, Ministry of Works and Development, New Zealand.

$$\text{or } \rho_s = 0.12 \frac{f'_c}{f_{yh}} \left(0.5 + 1.25 \frac{P_e}{\phi f'_c A_g} \right) \quad (2)$$

where P_e should be less than either $\phi 0.7 f'_c A_g$ or $\phi 0.7 P_o$. When rectangular hoops with or without supplementary cross ties are used, the total area of hoop bars and supplementary cross ties in each of the principal directions of the cross section within spacing s_h should be not less than the smaller of

$$A_{sh} = 0.3 s_h h'' \left(\frac{A_g}{A_c} - 1 \right) \frac{f'_c}{f_{yh}} \left(0.5 + 1.25 \frac{P_e}{\phi f'_c A_g} \right) \quad (3)$$

$$\text{or } A_{sh} = 0.12 s_h h'' \frac{f'_c}{f_{yh}} \left(0.5 + 1.25 \frac{P_e}{\phi f'_c A_g} \right) \quad (4)$$

where P_e should be less than either $\phi 0.7 f'_c A_g$ or $\phi 0.7 P_o$. The centre to centre spacing across the section between cross linked bars should not exceed the larger of one-third of the column cross section dimension in that direction or 200 mm when rectangular hoops are used.

Eqs. 1 to 4 are based on the SEAOC (4) recommendations modified to take into account the effect of axial load level. Eqs. 1 to 4 require less confining steel than the SEAOC recommendations when $P_e < 0.4 \phi f'_c A_g$, but more at higher axial load levels. The modification was based on the results of moment-curvature analyses conducted using idealized stress-strain curves for confined concrete (5,6), and from an assessment of the column test results reported in this paper. The greater confinement at higher axial load levels is necessary because of the greater depth of compressed concrete, and hence the greater dependence on the concrete.

COLUMN TEST UNITS

Fig. 1 shows the dimensions of the column test units. Each unit had a stub at mid-height which simulated a beam or pier cap. Four of the columns had an octagonal cross section with spiral reinforcement and four had a square cross section with two alternative arrangements of rectangular hoops. Tables 1 and 2 give the details of the columns, including the level of axial load applied during the tests. The actual quantities of spiral reinforcement present in Units 1, 3, 4 and 5 (for the higher axial load level) were 0.83, 0.83, 0.87 and 1.37 times that required by Eqs. 1 and 2, respectively. The actual quantities of rectangular hoop reinforcement present in Units 1, 2, 3 and 4 were 0.93, 0.90, 1.01 and 1.11 times that required by Eqs. 3 and 4, respectively. The central stub was reinforced so as to prevent failure occurring in that portion of the test unit.

The axial column load was held constant using a 10 MN capacity DARTEC servo-hydraulically controlled universal testing machine. The reversible horizontal load on the stub was applied by hydraulic jack which could be load or displacement controlled. The distribution of bending moment in the upper and in the lower half of each test unit was similar to that in a column between the face of an adjoining member and a point of contraflexure.

EXPERIMENTAL RESULTS

Typical measured horizontal load-displacement hysteresis loops are shown in Figs. 2 and 3. Cycles of horizontal loading of approximately to $\mu = \pm 2, \pm 4, \pm 6$ and sometimes ± 8 were applied. The "first yield" displacement was calculated assuming elastic cracked section behaviour up to the theoretical ultimate load, found using ACI column design charts (7) with the strength reduction factor ϕ taken as unity.

Unit 3 of the spiral column series suffered a shear/confinement failure immediately outside the confined plastic hinge region when μ was being increased from 4 to 6 (see Fig. 4). This indicated that the heavy confinement present in the plastic hinge region at high axial load levels enhances the concrete strength significantly and causes the plastic hinge region to spread along the column. The revised draft New Zealand Concrete Design Code specifies a longer potential plastic hinge region for heavily loaded columns, than for lightly loaded columns, as a result of this finding.

For the other columns of the series, very good stability of the load-displacement hysteresis loops was observed up to at least $\mu = \pm 6$ or ± 8 (Figs. 2 and 3 are typical) with very little strength degradation. Unit 5 of the spiral column series was cycled to $\mu = \pm 2, \pm 4, \pm 6$ and ± 8 with $P_e / F'_c A_c = 0.35$ before the load cycles shown in Fig. 2b were applied.

Dial gauges placed between steel yokes attached to the columns enabled strains and curvatures to be measured in the plastic hinge regions during the tests. The concrete compressive strains at which crushing of the cover concrete first became visible are listed in Tables 3 and 4 and range between 0.005 and 0.011, which is much higher than is normally assumed. Significant spalling of the cover concrete generally did not occur until $\mu = 4$ was being applied. However the concrete core remained well confined. The maximum compressive strains measured on the surface of the confined concrete core during tests are also listed in Tables 3 and 4 and range between 0.016 and 0.074. Although they are large they cannot be regarded as the "ultimate" concrete strains since much higher strains could have been reached had the loading been continued. It is of interest that the empirical expression of Corley (8) for the "ultimate" concrete strain gives values ranging between 0.22 and 1.10 times these measured maximum compressive strains. Tables 3 and 4 also show the maximum curvature ductility factor, ϕ / ϕ_y , measured at the critical plastic hinge sections. These ϕ / ϕ_y values range between 14 and 20 (disregarding spiral column Unit 3) and it is considered that all the columns could have reached $\phi / \phi_y = 20$ or greater had the loading been continued. Typical curvature distributions down the height of a spiral column are shown in Fig. 5. Fig. 6 shows the plastic hinge region of two columns after testing.

Although yielding of the transverse steel occurred during testing the confining action was adequately maintained. Therefore it does not seem justifiable to place more transverse steel in the column in an attempt to keep the confining steel stresses in the elastic range.

ULTIMATE MOMENTS AND LOADS

Tables 3 and 4, and Figs. 2 and 3, show the theoretical flexural

strengths calculated using the ACI column design charts (7) which assume $\epsilon_{cu} = 0.003$. The actual material strengths and $\phi = 1.0$ were assumed. The decrease in the theoretical ultimate load with increasing displacement shown in Figs. 2 and 3 is due to the P- Δ effect. The ACI method is seen to give a conservative result, particularly at high axial load levels. This discrepancy is a consequence of the enhancement in concrete strength due to confinement, and of strain hardening of the longitudinal steel at high strains. These factors can be taken into account in a refined flexural strength calculation.

It is commonly assumed (5,6) that for spiral columns the confined concrete strength f'_c is $f'_c + 4.1f_l$ where f_l is the lateral confining pressure exerted by the yielding spirals. For the spiral column Units 1 to 5 the confining pressure on this basis would have enhanced the concrete strength by 10 to 47%. Table 3 shows the theoretical moment capacities calculated assuming concrete core dimensions only, a rectangular concrete compressive stress block with constant stress f'_c over the full compressed region, an extreme fibre core strain ϵ_{cumax} as measured, and taking into account strain hardening of the longitudinal reinforcement. This theoretical ultimate moment capacity is assumed to occur at a distance of one-half of the compression block depth away from the central stub to account for the zone of influence of additional confinement from the stiff stub. Excellent agreement is observed in Table 3 between this theoretical moment and the experimental maximum moment measured at that section.

For the columns with rectangular hoops, the Kent and Park stress-strain curve (5) for concrete was modified to take into account the enhancement of concrete strength due to confinement. The maximum concrete stress was assumed to be Kf'_c where K is $1 + \rho_s f_{yh} / f'_c$. Fig. 7 shows the stress-strain model drawn to scale for the concrete confined by the rectangular hoops of Unit 3. Assuming concrete core dimensions only, a concrete compressive stress block as given by the modified Kent and Park relation, and taking into account strain hardening of the longitudinal reinforcing, the theoretical moment capacities calculated for extreme fibre concrete core strains of 0.005 and the maximum value measured in the tests, are compared in Table 4 with experimental moments measured at those strains. Again the agreement is reasonable. In this case the critical section has been taken to be in the column at the face of the stub. The agreement would have been better for the ϵ_{cumax} case had the critical section been taken at approximately one-half of the compression stress block depth away from the stub, since at that high strain the influence of the additional confinement from the stub would have become significant.

Analysis of the shear strength of the plastic hinge regions showed that well distributed longitudinal steel and closely spaced spiral steel increased the concrete shear capacity to well above that normally assumed in design.

CONCLUSIONS

The tests demonstrated that the quantity of confining steel recommended by the revised draft New Zealand Concrete Design Code in potential plastic hinge regions of columns results in very good concrete confinement. Displacement ductility factors generally greater than 6 were achieved by

the columns with only small degradation of flexural strength, and the hysteresis loops were relatively stable during cyclic loading. Significant enhancement in ductility and flexural strength occurs in columns well confined by spirals or rectangular hoops.

REFERENCES

1. Standards Association of New Zealand, "Draft Code of Practice for the Design of Concrete Structures", DZ3101, Wellington 1978.
2. Potangaroa, R.T., Priestley, M.J.N. and Park, R., "Ductility of Spirally Reinforced Concrete Columns Under Seismic Loading", Research Report 79-8, Department of Civil Engineering, University of Canterbury, Feb. 1979.
3. Gill, W.D., Park, R. and Priestley, M.J.N., "Ductility of Rectangular Reinforced Concrete Columns with Axial Load", Research Report 79-1, Department of Civil Engineering, University of Canterbury, Feb. 1979.
4. Structural Engineers Association of California Seismology Committee, "Recommended Lateral Force Requirements and Commentary", San Francisco, 1975.
5. Park, R. and Paulay, T., "Reinforced Concrete Structures", John Wiley and Sons, New York, 1975.
6. Park, R. and Leslie, P.D., "Curvature Ductility of Reinforced Concrete Columns Confined by the ACI Spiral", Sixth Australasian Conference on the Mechanics of Structures and Materials, Christchurch, Aug., 1977.
7. ACI Committee 340, "Ultimate Strength Design Handbook", Vol. 2, SP17-A, American Concrete Institute, Detroit, 1970.
8. Corley, W.G., "Rotational Capacity of Reinforced Concrete Beams", Journal of Structural Division, ASCE, Vol. 92, ST5, October 1966.

NOTATION

A_c	=	area of concrete core measured to outside of spiral or hoop
A_g	=	gross area of column section
A_{sh}^g	=	total effective area of hoop bars and supplementary cross ties in the direction under consideration at spacing s_h
f'_c	=	compressive cylinder strength of concrete
f'_c^c	=	confined compressive strength of concrete
f_y^{cc}	=	yield strength of longitudinal reinforcing steel
f_y^{yh}	=	yield strength of spiral, hoop or tie steel
h''	=	dimension of concrete core, at right angles to direction of hoop legs under consideration, measured to outside of peripheral hoop
P_e	=	maximum design compressive load due to gravity and seismic loading acting on column during an earthquake
P_o	=	axial load strength when load is applied with zero eccentricity
s_h^o	=	centre to centre spacing of spiral or hoop sets
ϵ_h	=	strain at extreme compression fibre of concrete
ϕ_{cu}	=	curvature, or strength reduction factor equal to 1.0 if the column design actions are such as to provide a high degree of protection against plastic hinging of columns, otherwise equal to 0.75
ϕ	=	curvature at first yield
ρ_s^y	=	ratio of volume of spiral or hoop reinforcement, including supplementary cross ties, if any, to volume of concrete core
ρ_t	=	ratio of area of longitudinal reinforcement to gross area of column
μ_t	=	displacement ductility factor defined as the ratio of the maximum horizontal displacement to horizontal displacement at first yield.

Table 1 Details of Column Units With Spiral Reinforcement

Unit	f'_c MPa	$\frac{P_e}{f'_c A_c}$ g	f_y MPa	Spiral Reinforcement			
				Dia. mm	f_{yh} MPa	Spacing ^a mm	ρ_s %
1	28.4	0.237	303	10	300	75	0.75
3	28.6	0.543	303	10	300	50	1.12
4	32.9	0.387	303	10	423	70	0.80
5	32.5	0.350	307	16	280	55	2.61
5 ^b	32.5	0.700	307	16	280	55	2.61

a. In the 600 mm long potential plastic hinge regions; spiral spacing was 120 mm elsewhere.
 b. Retested at a higher axial load level.
 Note: Longitudinal steel was sixteen 24 mm diameter deformed bars giving $\rho_c = 2.43\%$. Concrete cover to spiral = 20 mm.

Table 2 Details of Column Units With Rectangular Hoop Reinforcement

Unit	f'_c MPa	$\frac{P_e}{f'_c A_c}$ g	Hoop Reinforcement						
			Dia. mm	f_{yh} MPa	In Potential Plastic Hinge Region			Outside Plastic Hinge Region	
					No. of Hoop Sets	Spacing mm	ρ_s %	No. of Hoop Sets	Spacing mm
1	23.1	0.260	10	297	8	80	1.5	5	135
2	41.4	0.214	12	316	8	75	2.3	3	210
3	21.4	0.420	10	297	8	75	2.0	6	105
4	23.4	0.600	12	294	10	72	3.5	3	200

Note: Longitudinal steel was twelve 24 mm diameter deformed bars giving $\rho_c = 1.79\%$ with $f_y = 375$ MPa. Concrete cover to longitudinal steel = 50 mm

Table 3 Experimental and Analytical Results from Column Units With Spiral Reinforcement

Unit	Experimental Concrete Compression Strain ϵ_{cu}		Experimental Maximum ϕ_y	Flexural Strength kNm				
	First Visible Crushing	Maximum Measured ϵ_{cumax}		Maximum Experimental Moment M_{exp}	ACI with $\phi=1$		Using f'_c at ϵ_{cumax}	
					M_{theory}	$\frac{M_{exp}}{M_{theory}}$	M_{theory}	$\frac{M_{exp}}{M_{theory}}$
1	0.0074	0.056 ^a	25.4 ^a	890	723	1.23	886	1.01
3	0.0110	0.026 ^b	8.5 ^b	966	672	1.44	956	1.01
4	0.0094	0.048 ^a	16.3 ^a	1041	803	1.30	1096	0.95
5	0.0083	0.045 ^a	16.1 ^a	1079	807	1.34	1112	0.97
5 ^a		0.074 ^a	-	1276	564	2.26	1274	1.00

a. Average at $\mu = 8$ b. Average at $\mu = 4$

Table 4 Experimental and Analytical Results from Column Units With Rectangular Hoop Reinforcement

Unit	Experimental Concrete Compression Strain ϵ_{cu}		Experimental Maximum ϕ_y	Flexural Strength kNm					
	First Visible Crushing	Maximum Measured ^a ϵ_{cumax}		ACI with $\phi=1$		Using modified Kent and Park			
				M_{theory}	$\frac{M_{exp}^b}{M_{theory}}$	When $\epsilon_{cu} = 0.005$	At ϵ_{cumax}		
1	0.005	0.016	21	691	1.25	649	0.97	676	1.25
2	0.005	0.026	20	905	1.12	851	0.95	925	1.05
3	0.007	0.018	14	646	1.30	698	1.02	689	1.14
4	0.005	0.020	16	598	1.52	794	1.02	775	1.08

a. Measured at $\mu = 6$ or greater.
 b. M_{exp} is maximum moment measured.
 c. M_{exp}^c is moment measured when $\epsilon_{cu} = 0.005$.
 d. M_{exp}^d is moment measured when ϵ_{cumax} is reached.

Note: 1 mm = 0.0394 in, 1 MPa = 145 psi, 1 kNm = 0.737 kip ft

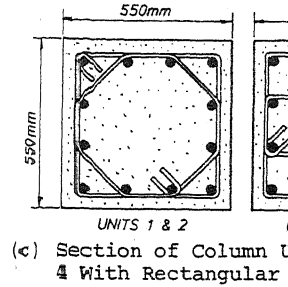
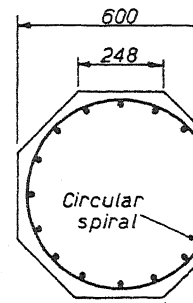
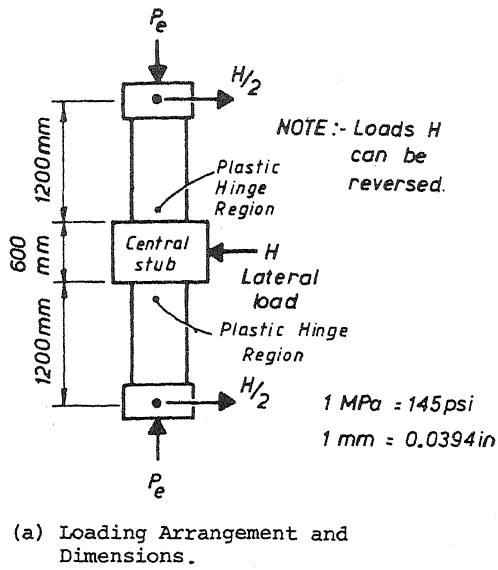


Fig. 1 Dimensions, Reinforcing Arrangements and Loading of C Test Units.

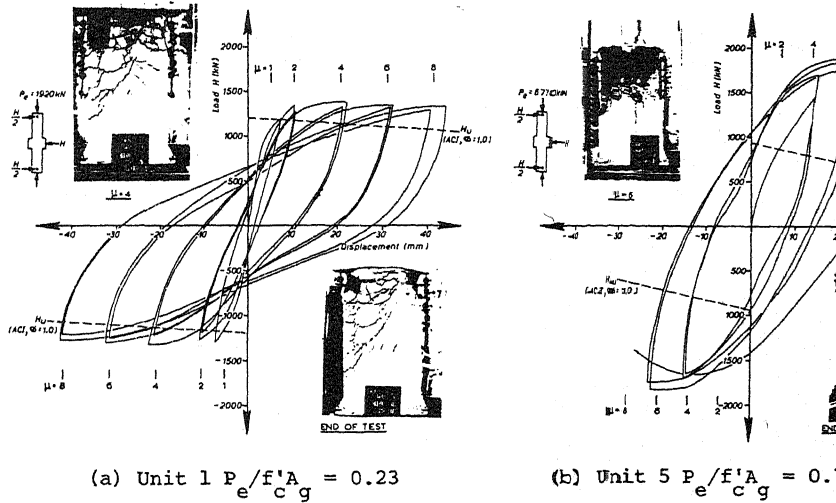
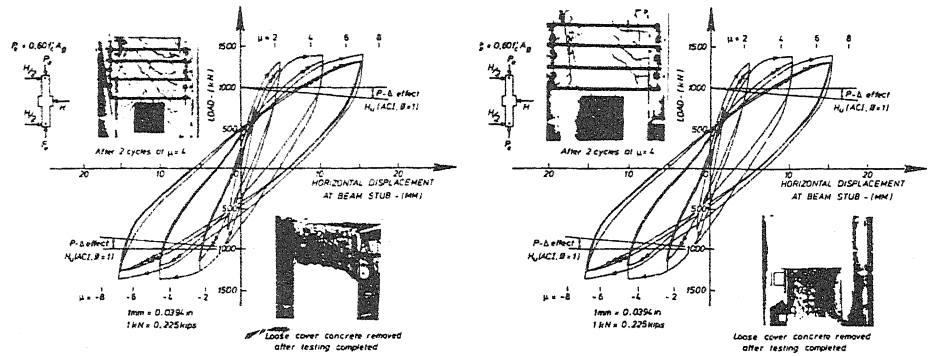


Fig. 2 Measured Horizontal Load-Deflection Loops and Observed Damage to Two Columns With Spirals.



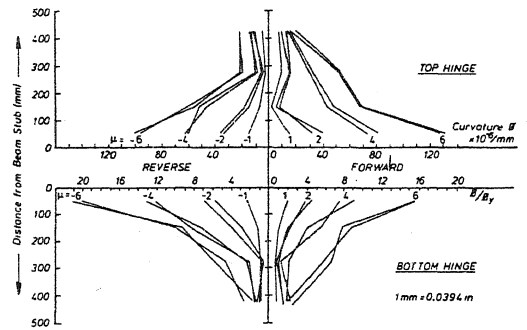
(a) Unit 1 $P_e/f'_c A_g = 0.26$

(b) Unit 4 $P_e/f'_c A_g = 0.60$

Fig. 3 Measured Horizontal Load-Displacement Loops and Observed Damage of Two Columns With Rectangular Hoops.

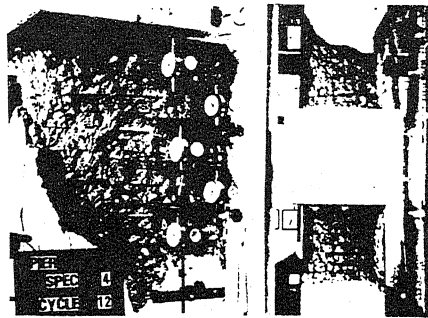


Fig. 4 Failure of Spiral Unit 3 Outside Plastic Hinge Region.



(a) Unit 1

Fig. 5 Measured Curvature Distribution Down Column for Unit 1 Column With Rectangular Hoops.



(a) Spiral Unit 4 (b) Hooped Unit 3

Fig. 6 Plastic Hinge Regions at End of Test.

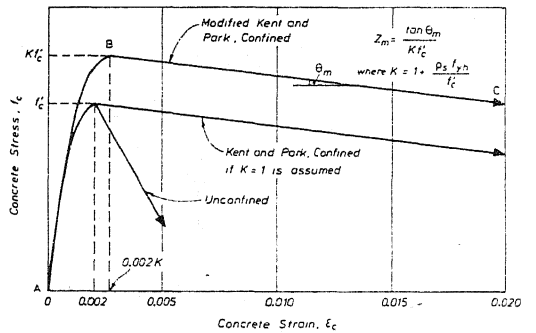


Fig. 7 Model for Stress-Strain Behaviour of Concrete Confined by Rectangular Hoops.